From methods to meaning in functional neuroimaging

Reinders, Antje Annechien Talea Simone

4

Inter-scan displacement induced variance in PET activation data is excluded by a scan specific attenuation correction

Authors:
A.A.T.S. Reinders, A.T.M. Willemsen, J.R. Georgiadis
M. Hovius, A.M.J. Paans, J.A. den Boer

(Published in: NeuroImage 2002; 17(4): 1844-1853)

Abstract

In PET activation studies, linear changes in regional cerebral blood flow may be caused by subject inter-scan displacements rather than by changes in cognitive state. The aim of this study was to investigate the impact of these artifacts and to assess whether they can be removed by applying a scan-specific calculated attenuation correction (CAC) instead of the default measured attenuation correction (MAC). Two independent data sets were analyzed, one with large (data I) and one with small (data II) inter scan displacements. After attenuation correction (CAC or MAC), data were analyzed using SPM99. Inter scan displacement parameters (IDP), obtained during scan realignment, were included as additional regressors in the general linear model and their impact was assessed by variance statistics revealing the affected brain volume. For data I, this volume reduced dramatically from 579 cm^3 to 12 cm^3 (approximately 50 fold) at $p_{uncorr} \leq 0.001$ and from 100 cm^3 to 0 cm^3 at $p_{corr} \leq 0.05$ when CAC was applied instead of MAC. Surprisingly, for data II, applying CAC instead of MAC still resulted in a substantial (approximately ten fold) reduction of the affected volume from 23 cm^3 to 2 cm^3 at $p_{uncorr} \leq 0.001$. We conclude that inter scan displacement induced variance can be prevented by applying a (re-)aligned attenuation correction scan, e.g. CAC. With MAC data, introducing IDP covariates is not an alternative since they only model this variance. Even in data with minor inter scan displacements, applying a (re-)aligned attenuation correction method, e.g. CAC, is superior to a non aligned MAC with IDP covariates.

Introduction

Regional cerebral blood flow (rCBF) is coupled to neuronal activation. Therefore, changes in neuronal activation, for example due to performing a specific task, will induce a change in rCBF which can be measured by positron emission tomography (PET). A PET activation study consists of several acquisitions for each of the task conditions.

In PET, the assessment of the radioactivity distribution is based on the coincidence detection of two opposite 511-keV photons emerging from a single positron-electron annihilation. To obtain a quantitative image, the measured data must be corrected for dead time, random coincidences, scattered radiation, and attenuation. Dead-time and random coincidences are measured during data acquisition by monitoring the single count rates in the individual detector blocks (dead time) and by a delayed coincidence measurement (accidental coincidences) (Hoffman et al., 1981). Attenuation correction is usually performed on the basis of a transmission scan obtained using 511-keV coincidence photon sources. The measured attenuation scan is count-limited, which results in attenuation correction

factors that have significant statistical noise, which subsequently propagates as added noise in the reconstructed PET images (Huang et al., 1979; Meikle et al., 1993; Weinzapfel and Hutchins, 2001). The scatter correction is based on the individual attenuation map according to the procedure as described by Watson et al. (1997).

Misalignment of the transmission scan with the emission scan will cause artifacts and/or reduce the quality of PET activation studies. This is in accordance with Huang et al. (1979), who stated that unpredictable artifacts in the reconstructed PET images emerge from subject inter scan displacement between the transmission scan and the multiple emission scans in a brain activation imaging sequence. In many applications, small alignment errors between transmission and emission scans have little effect. However, PET activation studies investigate very small changes in rCBF over many scans in which even a small misalignment may cause unpredictable artifacts in the analysis results. In these studies realignment between blood flow images is rigorously addressed, correcting for subject displacement but this does not reduce the artifacts resulting from the transmission-emission mismatches.

Previously, after investigating scan order and inter scan displacement effects, Brett et al. (1999) found that linear changes in signal across the scanning sessions may be caused by inter scan displacement artifacts rather than changes in cognitive state, e.g. attention. They found a strong relationship between scan order and inter-scan displacement parameters which "raised the possibility that the effects may be movement rather than time related." This idea was strengthened because artifacts could be reproduced merely by applying misaligned attenuation correction. Brett et al. (1999) speculated that the artifacts may cause difficulties in interpretation of studies with unbalanced conditions across scan order or when subject inter scan displacement is related to activation condition.

Thus, it should be possible to model artifacts originating from the misalignment between the emission scans and the measured attenuation scan by including inter-scan displacement parameters (IDP) (three translations, three rotations), obtained during scan realignment (Friston et al., 1995a), as additional regressors in the general linear model (GLM) (Friston et al., 1995b). The model fit is optimal in the least-squares sense for explaining the variance in functional imaging data. The significance of the variance explained by the regressors, i.e. IDP, can be assessed by variance statistics, i.e. F statistics. Brain areas in which variance is explained by the IDP are brain areas contaminated by transmission emission scan mismatch artifacts.

By performing a scan-specific calculated attenuation correction (CAC) rather than using the measured attenuation correction (MAC), which is measured only once, misalignment between transmission and emission scans can be rigorously addressed. A CAC can replace MAC when the attenuation is near uniform, e.g. the head. A common straightforward method (Phelps et al., 1975; Bergström et al.,

1980) is to place an ellipse on each image about the contour of the head and to calculate the attenuation along each detector-pair line-of-response (LOR) for each ellipse. Other methods, like re slicing attenuation data with transformation parameters obtained from realignment of emission data (Andersson et al., 1995), edge detection algorithms (Siegel and Dahlbom, 1992), maximum-likelihood reconstruction of attenuation and activity (Nuyts et al., 1999), or automated attenuation correction models (Weinzapfel and Hutchins, 2001) can also be applied.

The aim of this study was to investigate whether the variance as modeled by the inter scan displacement parameters is actually the result of a small (time-varying) mismatch of the emission scans and the measured attenuation scan and to investigate the impact of these artifacts on functional neuroimaging studies. It was hypothesized that, in the case of calculated attenuation corrected emissions scans, the variance explained by the IDP should be reduced substantially.

Methods

Data sets from two different activation studies were analyzed. All measurements were performed after informed consent and were approved by the medical ethics committee of the Groningen university hospital. For both data sets the subjects were placed in the gantry and were positioned by aligning the standard low power laser beams.

In the first data set (data I), ten subjects underwent four conditions of increasing traumatic fear (1-4) which were obtained twice, resulting in eight scans. Data I is a study with unbalanced conditions across scan order (always 1,2,3,4,3,4,1,2). To minimize disturbance of subjects it was decided not to reposition them between scans, and a head-restraining adhesive band was used only when it did not frighten the subjects. Subsequent realignment procedures performed in SPM99 (see data preprocessing) showed that these subjects had moved considerably between sessions (see results). To maximize the search volume for which statistical tests could be performed, scans with major non scanned brain parts were discarded after visual inspection of the images by two independent observers. Three scans with observed intra scan motion during the PET data collection and one scan containing a procedural error were also excluded from the analyses. For the ten subjects in total 15 scans were excluded, leaving 65 scans for the statistical analyses.

The second data set (data II) included four subjects undergoing two randomized conditions of auditory stimulation and vocalization, which were repeated six times resulting in twelve scans per subject. Since the main effect of interest was located in the brainstem a large bounding box was used during normalization. One subject was positioned high into the PET camera, causing the upper slices not to be available for the analysis. After normalization the scans were masked to

exclude nasal activation, probably caused by an increased nasal blood flow during vocalization. For this group of subjects, inter scan displacement was minimized by repositioning the subject before each scan using head markings and the laser positioning system of the PET camera. The head-restraining adhesive band was used on all subjects.

Data acquisition

All scans were performed using a Siemens ecat exact HR+ PET scanner, which acquires 63 slices simultaneously over an axial length of 15.5 cm. Before emission scanning an attenuation scan was performed using the three internal rotating 68Ge/68Ga rod sources. The PET scans were performed after a bolus injection of a fixed dose of 500 MBq of $H_2{}^{15}O$ for each scan in 3D acquisition mode. The tasks started at the moment of injection and continued during the scanning period. Each PET data acquisition run consisted of two frames, first a 30 seconds background correction frame followed by a 120 seconds perfusion scan. The interval between two scans was set at ten minutes to allow for decay. Data were corrected for scatter, decay, and dead time. After data collection the data underwent different processing steps, which are schematically shown in the flow-diagram (figure 4).

Image reconstruction

The emission scans of both data sets were reconstructed using the standard filtered back-reconstruction algorithm in brain mode with a zoom of 2.25 and a Gaussian filter of 4.0 mm FWHM (full width at half maximum). The reconstructed spatial resolution was 5.7 mm. For both data sets attenuation correction was performed in two ways, i.e. MAC and CAC, resulting in four data sets (data I, MAC and CAC data; data II, MAC and CAC data). For MAC, the measured attenuation scan was used for attenuation correction. For CAC, separate ellipses were drawn manually on the non-attenuation-corrected images, assuming default attenuation values for bone and tissue and a bone thickness of 4.5 mm.

Data preprocessing

The 1999 version of statistical parametric mapping (SPM99) software was used for spatial transformation (realignment, normalization and smoothing) and statistical analysis of the data (Friston et al., 1995a,b; Talairach and Tournoux, 1988). Two lines of analysis were followed as shown in figure 4. The first main line (MAC and CAC, figure 4) of investigation is the standard independent preprocessing of MAC and CAC data, as is performed in normal practice. The second line (MAC-d, figure 4) of investigation is the dependent preprocessing line.

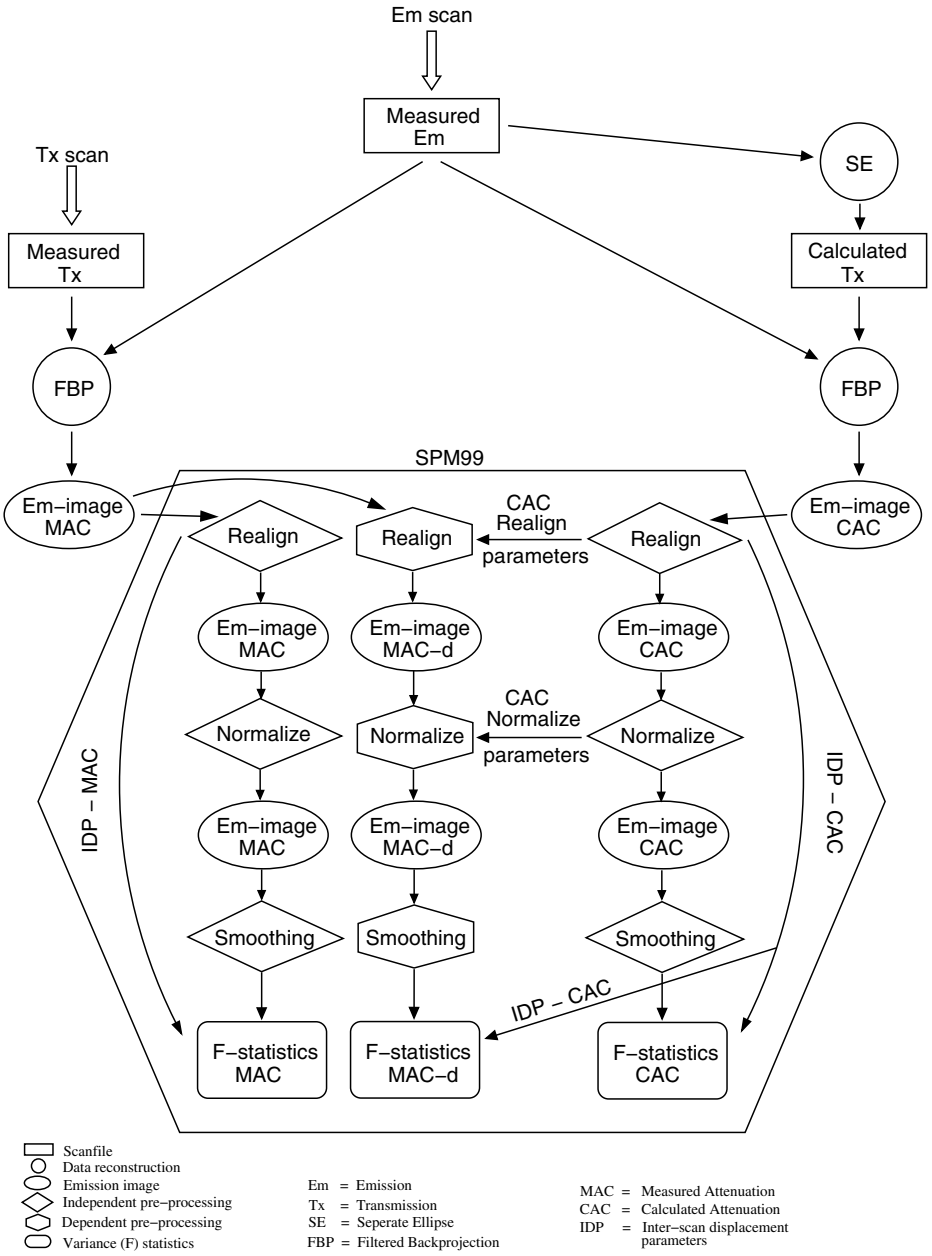

Figure 4.1: *Caption on next page*

Figure 4.1: *Schematic representation of the different processing steps each data set underwent after data collection. The main processing steps are data reconstruction including attenuation correction (FBP), realignment and normalization. The resulting emission images were finally smoothed and statistically analyzed. The left and right columns show the processing of the original data with either a measured attenuation correction (MAC) or a calculated attenuation correction (CAC). This is the first line of preprocessing, the independent preprocessing of MAC and CAC data as performed in normal practice. The central column represents the dependent processing of the MAC data (MAC-d), the realignment and normalization use the parameters obtained from the CAC data. This is the second line of preprocessing.*

The four data sets (see above) were translated to the Analyze (SPM99 uses the simple header and flat binary image file format of ANALYZE7 (Mayo clinic, Rochester, USA. www.mayo.edu/bir/), with slight customizations to the header) data format and the origins were manually set at the anterior commissure. Then the PET time series were realigned to the mean to correct for inter subject head displacements in terms of translations and rotations. Hereafter, all the scans were transformed into a standard stereo-taxic MNI space (Friston et al., 1995a) using 7x8x7 nonlinear basis functions and heavy regularization during the normalization procedure. As a final step in the preprocessing, data was spatially smoothed using an isotropic Gaussian kernel of 10 mm FWHM. The final spatial resolution was 11.5 mm.

For each data set the IDP, consisting of three translations and three rotations obtained during scan realignment, of each image and of each subject were recorded for subsequent inclusion in the model definition (see below). Note that in the standard independent preprocessing case, the IDP obtained from MAC and CAC data will not be identical and will be referred to as IDPmac and IDPcac.

Above, the MAC and CAC reconstructed data were independently realigned and normalized. However, since the type of attenuation correction influences the data, which in turn determines the realignment and normalization, the realignment and normalization parameters will not be identical. Therefore, changes in variance explained by the model parameters may reflect not only differences in attenuation correction but also changes in the preprocessing. To exclude the latter contribution, the MAC data were also realigned and normalized using the parameters as obtained during realignment and spatial normalization of the CAC data and is therefore dependent on the CAC parameters (MAC-d, figure 4). The CAC reconstruction method was assumed to be superior (see introduction).

Data modeling and analyses

For functional neuroimaging data SPM is widely used to assess activation patterns in brain activation studies. The data are modeled using the general linear model (GLM), consisting of multiple univariate regression analyses. These model fits are optimal in the least square-sense for explaining the observed variance. The significance of the variance explained by the regressors in the model can be assessed by F statistics and displayed as an F SPM.

To investigate the amount of variance that can be explained by the IDP, they were included as additional regressors in the separate SPM99 design matrices for data sets I and II. The IDPcac were included for CAC data and the IDPmac for the independent preprocessed MAC data. To assess the influence of attenuation correction on the pre-processing steps, the IDPcac were also included for the dependent MAC data (MAC-d). To investigate linear changes in signal across the scanning session a scan-time covariate (the scan-time parameter (SP)) was defined containing the initiation time of the scan, which is similar to the scan order covariate from Brett et al. (1999), but gives a more precise definition of time between scans. This is of specific importance for data I in which scan interval times varied considerably.

Variance explained by SP, by IDP, or by both were assessed by variance statistics (F map). The variance explained by the 6 IDP together was used as a measure for the effect of a mismatch between emission and attenuation data. SPMs were inspected at the conventional threshold of $p \leq 0.05$ corrected for multiple comparisons (p_{corr}). Additionally, the SPM's were explored at a liberal threshold of $p \leq 0.001$ uncorrected for multiple comparisons (p_{uncorr}). This threshold is commonly used in imaging studies to identify areas included in the *a priori* hypothesis (Friston et al., 1991) from which the corrected significance level (p_{corr}) can subsequently be obtained using a small volume for multiple testing, i.e. small-volume correction (SVC). These areas can also be contaminated by mismatch artifacts.

Three models were set up to test mismatch artifacts and linear time effects. In the first model only SP was included as an extra parameter, the 'SP' model. The second model included only the 6 IDP to model inter-scan displacement artifacts, the '6 IDP' model. The third model combined the 6 IDP and the SP, the '6 IDP + SP' model.

In addition the mean, standard-deviation, and correlation (r^2, with SP) for each of the 6 IDP were calculated separately for both IDPmac and IDPcac of data sets I and II. Furthermore, the amount of variance in SP, which could be explained by the 6 IDP, was investigated using a linear least-square fit, again separately for each of the four cases. This least square-fit was calculated independent of the PET activation data and the conditions, with only SP as the response variable and the 6 IDP as predictor variables.

Results

Data I

Data I is the study with unbalanced conditions across scan order and inter scan subject displacement, which is related to activation condition. Figure 4.2 (left) shows a typical example of the translations required to reposition the consecutive scans to the position of the first scan for a subject in data set I. Considerable inter scan displacements can be observed.

Inter-scan displacement and scan-time parameter

Table 4.1 A) presents the mean, standard-deviation, and correlation of each IDP for data set I using either MAC or CAC. Correlation analyses with the SP showed that the translation over the y axis shows the highest but still very low value of $r^2 = 0.13$ (CAC) and $r^2 = 0.15$ (MAC). Using a linear least-square fit it was shown that IDP could explain only 20.5% (CAC) and 21.5% (MAC) of the scan-time variance.

Inter scan displacement-related variance in the PET data

As shown in table 4.2 A) for the CAC case no voxels were found in which a significant amount of variance was explained by either of the three models at the $p_{corr} \leq 0.05$ threshold. At the more liberal threshold of $p_{uncorr} \leq 0.001$ in all three models a relatively small number of voxels were found for which a significant amount of variance was explained by the model parameters.

Table 4.2 A) shows that for the MAC case the number of voxels in which a significant amount of variance is explained by the model parameters included is very large with the 6 IDP (12568 voxels) and 6 IDP + 1 SP (10100 voxels) models. This represents brain volumes of 100 cm^3 and 81 cm^3 respectively ($p_{corr} \leq 0.05$). At the liberal threshold ($p_{uncorr} \leq 0.001$) 72403 voxels (a brain volume of 579 cm^3) with the 6 IDP model and 67650 voxels (a brain volume of 541 cm^3) with the 6 IDP + 1 SP model for which identified where a significant amount of variance was explained by the model parameters included. In contrast, only a relative small number of voxels were identified for which a significant amount of variance could be explained by the SP in the SP only model at this threshold. From table 4.2 A) it is apparent that the main effect in data set I is caused by the IDP covariates (see also discussion). The corresponding projections (F maps) of the contaminated volume are shown in figure 4.3.

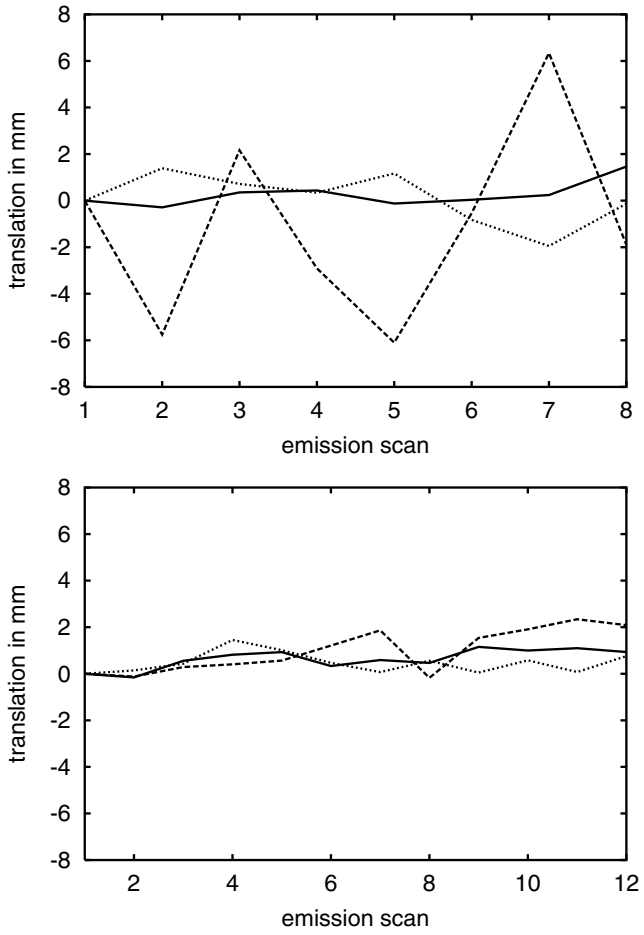

Figure 4.2: *Results of the SPM realignment procedure. Two typical examples are depicted (one subject for each data set) of the translations over the x (dotted), y (solid) and z (dashed) axis, as required to reposition the consecutive scans to the position of the first scan. On the left, the study with unbalanced conditions across scan and without repositioning of subjects between scans (Data I) is shown. Considerable inter scan displacements, particularly in the z direction, can be observed. On the right the inter scan displacement for the study with randomized conditions and minimized inter scan displacements (Data II) is shown. A rather limited inter scan displacement is apparent.*

Table 4.1: *Mean, standard-deviations (s.d.) (in mm c.q. radians) and correlation with scan-time (r^2), of the six realignment parameters for two data sets using two types of attenuation correction i.e. CAC and MAC.*

		translation			rotation		
		x	y	z	pitch	roll	yaw
A) Data set I							
CAC	mean	-0.38	0.74	-1.62	0.00	-0.01	0.00
	s.d.	1.79	1.11	5.33	0.04	0.02	0.04
	r^2	0.10	0.13	0.04	0.00	0.03	0.05
MAC	mean	-0.34	0.60	-1.25	0.00	-0.01	0.00
	s.d.	1.48	0.86	4.25	0.03	0.02	0.03
	r^2	0.10	0.15	0.04	0.00	0.06	0.05
B) Data set II							
CAC	mean	-0.27	0.78	-0.62	0.02	0.00	0.00
	s.d.	0.92	0.62	3.38	0.02	0.01	0.01
	r^2	0.08	0.07	0.15	0.00	0.00	0.11
MAC	mean	-0.31	0.55	-0.57	0.02	0.00	0.00
	s.d.	0.81	0.42	2.97	0.02	0.01	0.01
	r^2	0.08	0.01	0.09	0.00	0.00	0.11

CAC = calculated attenuation correction
MAC = measured attenuation correction

Data II

Data II is the study with randomized conditions and minimized inter scan displacements. Figure 4.2 (right) shows a typical example of the translations required to reposition the consecutive scans of a subject in data set II. This figure shows that in this data set, a rather limited inter scan displacement is apparent.

Inter scan displacement and scan-time parameter

Table 4.1 B) presents the mean, standard deviation, and correlation of each IDP for data set II using either CAC or MAC. After correlation analyses with the SP the translation over the z axis shows the highest but still very low value of r^2 = 0.15 for CAC parameters. For the MAC parameters the third rotation (yaw) showed the highest value of r^2 = 0.11. Using a linear least-square fit it was shown that IDP could explain only 21.1% (CAC) and 15.6% (MAC) of the scan-time variance.

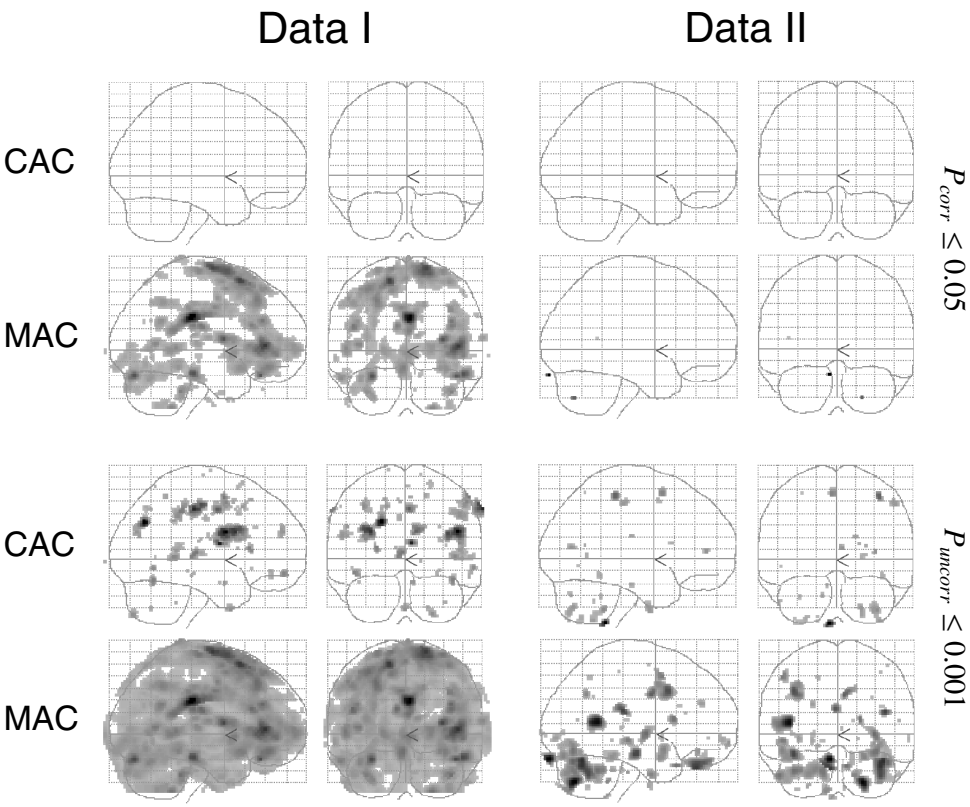

Figure 4.3: *F maps, assessed using the F statistics in SPM, showing the brain volume for which a significant amount of variance is explained by the six realignment parameters at two thresholds for data sets I and II. The upper two rows show voxels surviving the $p_{corr} \leq 0.05$, the bottom two rows show voxels surviving the liberal threshold of $p_{uncorr} \leq 0.001$. The first and second columns depict the sagittal and coronal projections of variance which is explained by the six realignment parameters for data I, while the third and the fourth columns present the variance which is explained by the six realignment parameters for data II. The rows show the different attenuation corrections (CAC, calculated attenuation correction, MAC, measured attenuation correction).*

Table 4.2: *The total number of voxels in which a significant amount of variance is explained by the covariates for two data sets. Three models were used to model the data, including the SP only, including the 6 IDP parameters only or including both. In the latter case the explained variance was determined for all seven parameters (6 IDP + SP) together as well as for the constituting 6 IDP and the SP separately. The number of voxels are obtained by an F test on the covariates and thresholded at $p \leq 0.001$ uncorrected and $p \leq 0.05$ corrected for multiple comparisons.*

			6 IDP + 1 SP		
	1 SP	6 IDP	IDP + SP	IDP	SP
A) Data set I					
$p_{corr} \leq 0.05$					
CAC	0	0	0	0	0
MAC	38	12568	10100	7935	0
MAC-d	31	14093	12272	10812	0
$p_{uncorr} \leq 0.001$					
CAC	759	1494	1277	985	200
MAC	5353	72403	67650	63465	399
MAC-d	4521	65990	61834	58991	548
B) Data set II					
$p_{corr} \leq 0.05$					
CAC	0	0	0	0	0
MAC	0	6	2	4	0
MAC-d	0	0	0	0	0
$p_{uncorr} \leq 0.001$					
CAC	617	263	438	71	1001
MAC	690	2841	2885	2725	506
MAC-d	947	2178	2440	2333	1017

CAC = calculated attenuation corrected
MAC = measured attenuation corrected
MAC-d = MAC dependently pre-processed
SP = scan-time parameter
IDP = inter-scan displacement parameters

Inter scan displacement related variance in the PET data

As shown in table 4.2 B) at the threshold of $p_{corr} \leq 0.05$ there is no difference between CAC or MAC data, i.e., the volume in which a significant amount of variance is explained by either of the three models is negligible. However, the liberal threshold ($p_{uncorr} \leq 0.001$) identified brain regions which were contaminated by mismatch artifacts, even though inter scan displacement was minimized. A total

of 263 voxels (a brain volume of 2 cm^3) with the 6 IDP only model and of 438 voxels (a brain volume of 3 cm^3) with the 6 IDP + 1 SP model were found in the CAC data. For the MAC data 2841 voxels (a brain volume of 23 cm^3) with the 6 IDP only model and 2885 voxels (a brain volume of 23 cm^3) with the 6 IDP + 1 SP model contained variance which could be explained by the model parameters included.

Volume in which a significant amount of variance is explained by the SP model parameter does not differ much between the SP only model and the 6 IDP + 1 SP model (MAC, $p_{uncorr} \leq 0.001$, table 4.2 B)), i.e., no linear inter scan displacement over time could be observed in these data. With the SP only model, only a negligible difference in volume of 0.5 cm^3 was identified between CAC and MAC data (617 versus 690 voxels, i.e. 4.9 cm^3 versus 5.5 cm^3) at the $p_{uncorr} \leq 0.001$. From table 4.2 B) it is apparent that the main effect in data set II is again caused by the IDP covariates (see also discussion). The corresponding projections (F maps) of the affected brain volume are shown in figure 4.3.

Influence of preprocessing

In the dependently preprocessed MAC data (MAC-d), according to the scheme in figure 4, artifacts are still present in both data sets I and II. The number of voxels in which a significant amount of variance is explained by either of the three models is different but on the same order of magnitude in the independent preprocessed MAC and the dependent preprocessed MAC (see table 4.2 A) and B)).

Discussion

The retrospective realignment of consecutive scans ensures that all images in a series are in the same spatial orientation. Although this realignment between blood flow images corrects the rCBF images for subject displacement between scans, it does not reduce the artifacts originating from a misalignment between emission and transmission scan. One obvious approach to minimizing such a misalignment is to reposition the subject before each scan. This has the additional advantage of maximizing the brain volume for statistical analyses. However, not all between scan motions are easily discernible and misalignment artifacts may evolve, particularly due to rotations of the head. For example, if subjects pitch their head, a displacement may not be observed. This may be an explanation for the increase in signal in the frontal lobe (shifting into the scanner range) and a decrease in signal in the occipital regions (shifting out of the scanner range) found by Brett et al. (1999). These kinds of artifacts are time related (pitching the head over time), so it may be possible to model these artifacts by scan order instead of inter scan displacement, as they showed.

Andersson et al. (1995) reconstructed emission scans without attenuation correction and realigned all scans onto the first scan (assumed to be correctly aligned with the transmission scan). On the basis of the measured attenuation scan, a procedure was applied to yield new attenuation data for correctly reconstructing the emission scans. This method also corrects for subject motion, but still requires a transmission scan with its often rather low signal-to-noise ratio (Ollinger, 1992; Meikle et al., 1993). To improve the signal to noise ratio of a measured attenuation scan, the attenuation scan can be segmented (Bettinardi et al., 1999; Zaidi et al., 2002). This method, however, can suffer from an erroneous segmentation. As already mentioned in the introduction other methods like edge detection algorithms (Siegel and Dahlbom, 1992) maximum-likelihood reconstruction of attenuation and activity (Nuyts et al., 1999), or automated attenuation correction models (Weinzapfel and Hutchins, 2001) can also be applied to address misalignment between transmission and emission scans. For this investigation we used CAC as obtained by drawing ellipses. This method reduces total scan duration and is therefore more comfortable for subjects. Furthermore with a CAC, the attenuation correction is noise free by default, which is not the case with a MAC (Weinzapfel and Hutchins, 2001). However, CAC may suffer from errors, which are subject specific (different head shape and skull thickness), as well as operator dependent (manual procedure). Note that this may introduce additional variance which must be explained by the model. If so, the CAC results as reported in table 4.2 are probably an underestimation of the true effect of aligning the attenuation scan to the emission scans. Nevertheless, a detailed discussion of the (dis)advantages of the various methods is beyond the scope of this chapter. For the results as discussed here, it is essential that the attenuation and emission scans were properly aligned, which was adequately achieved with CAC.

Comparing data sets I and II, it is apparent that the volume for which IDP explains a significant amount of variance is much larger for data set I. This was expected since in data set I repositioning of the subjects between scans was not possible, resulting in larger between-scan displacements (table 4.1 A)). Application of CAC instead of MAC for data set I dramatically reduced (approximately 50 fold (from 579 cm^3 to 12 cm^3) at $p_{uncorr} \leq 0.001$) the brain volume for which IDP explained a significant amount of variance (table 4.2). The affected brain volume is confluent and widespread through gray and white matter, i.e. more sensitively detectable with wider smoothing kernels, excluding the possibility of being task-related. This clearly demonstrates that the variance explained by the IDP is caused by the misalignment between the measured attenuation scan and the consecutive emission scans. This confirms the speculation of Brett et al. (1999) that "scan order effect is in fact an artifact of movement across the scanning session" after they reproduced scan order effect by applying misaligned attenuation correction. Even when applying CAC on data I, the remaining volume for which variance was explained by IDP (at $p_{uncorr} \leq 0.001$) is still considerable, showing that for data

sets with larger inter scan displacements, the introduction of IDP as additional regressors into the GLM of SPM should still be considered.

Surprisingly, even for data set II, for which subjects were repositioned between each scan, the application of a calculated attenuation correction, as compared to the measured attenuation correction, still resulted in a ten fold reduction (23 cm^3 versus 2 cm^3 at $p_{uncorr} \leq 0.001$) of the volume for which a significant amount of variance was explained by IDP. This is consistent with data of Brett et al. (1999), who found highly significant effects in data of normal subjects. These findings are counter intuitive and strongly suggest that even in the case of data II, small differences in the alignment between transmission and emission scans are present, resulting in additional scan-specific variance in the data which are to be modeled during the analysis.

The results for the different models as presented in table 4.2, should be interpreted with caution as they are based on different levels of statistical power due to a difference in degrees of freedom. Nevertheless, despite the lower degrees of freedom, the volume for which IDP explained a significant amount of variance is much larger than the volume for which SP explained a significant amount of variance. The only exception was for data set II at $p_{uncorr} \leq 0.001$ with CAC, when comparing the SP model with the 6 IDP model. However, the difference in volume for which a significant amount of variance is explained in the SP only model is negligible between CAC and MAC data (4.9 cm^3 versus 5.5 cm^3) and is therefore not a function of the attenuation method. This phenomenon is also observed in the model which combines the 6 IDP and the SP covariates and is supported by the low correlations between SP and the six IDP as presented in table 4.1. This indicates that, for data II, the variance explained by SP is mainly an actual scan-order effect rather than an artifact induced by between scan displacements.

The generally small overlap between the volumes found for SP and IDP is not consistent with Brett et al. (1999), who found dramatic reductions in the variance explained by scan order after inclusion of the IDP. We could not find a similar relation between scan order and IDP, only a trend was noticed in data I (see table 4.2 A). This is not surprising since the variance in the scan time which could be explained by IDP was only 22% or less for our data. Also the correlation between IDP and scan-time showed a very low correlation value of maximal $r^2 \leq 0.15$ (table 4.1 A)). Thus, in our case, scan order is not a good prediction of displacement related-artifacts.

These results clearly show that aligning the transmission and emission scans, e.g. by applying a CAC, is essential, even when subjects are carefully repositioned between scans. Particularly, the application of a non aligned MAC and the introduction of IDP parameters into the SPM model to account for possible displacement related artifacts should be discouraged. From the large difference in the brain volume between MAC and CAC, for which a significant amount of variance

is explained by the IDP (table 4.2 A) and 4.2 B)), it is concluded that IDP mainly model inter scan displacement related variance. Nevertheless, IDP attempt only to model the artifacts originating from incorrect attenuation correction, but cannot remove them. Moreover, including the six IDP requires special care, because in the case of stimulus-correlated movement they might explain some of the variance of interest. However, our results indicate that if the attenuation and emission scans are aligned, e.g. with CAC, the six IDP need not be included in the statistical model. This also saves six degrees of freedom, thereby improving the statistical power of PET activation studies, which have generally a limited number of degrees of freedom. In addition, using an aligned attenuation correction enables a better assessment of linear changes in rCBF across scanning sessions (scan order effects), since SP will no longer be contaminated by mismatch artifact related variance. Still, repositioning the subject is important to maximize the brain volume being scanned.

The relative contributions of the consecutive steps in the preprocessing of SPM were investigated by dependent pre-processed MAC data using parameters identical to those for the CAC data. Considering the small differences in the volume for which a significant amount of variance is explained (MAC versus MAC-d, table 4.2 A), and 4.2 B)), it can be concluded that the mismatch between transmission and emission scans has little effect on the realignment and normalization procedures. This is not surprising since these procedures are based on the overall activity in the total brain volume, whereas the aim of PET activation studies is to model the (small) changes in the activity distribution. To investigate the real amount of mismatch contamination, the IDPcac were included as additional regressors in the GLM for analyzing the MAC-d data. Assessing these variance statistics should reveal the real variance explained by mismatch contamination without any influence of differences in the relative contributions of consecutive preprocessing steps. The number of voxels in which variance is explained by either of the three models is different but on the same order of magnitude as in the independent preprocessed MAC data with IDPmac (table 4.2 A and B: MAC and MAC-d). Since the difference between both is that the latter uses the design matrix of the CAC data, it follows that the differences in the design matrix have little effect on the analysis. Therefore, changes in IDP covariates, due to differences in the activation signal (MAC versus CAC), do not explain the main effect seen in this study. If we now compare the MAC-d and CAC case, a very large difference is observed in the volume in which a significant amount of variance is explained by either of the three models. Since the design matrices are now identical, it follows that the differences in volume are indeed related to the method of attenuation correction and not to the design-matrix. Therefore, it can be concluded that the reported artifacts are indeed caused by the mismatch between the (measured) transmission scan and the emission scans.

In conclusion, even minor displacements between scans will result in a mismatch between the measured transmission and consecutive emission scans, resulting in considerable additional scan-specific variance which must be explained by the SPM model. Although introduction of the inter scan displacement parameters as covariates into the SPM analyses may (partly) model this additional variance, it cannot remove this variance, but it will reduce the statistical power. In contrast, this variance can be prevented by applying a (re)aligned attenuation correction scan, e.g. CAC. Therefore, addressing the misalignment between transmission and emissions scans is essential in rCBF PET activation studies.

Acknowledgments

The authors wish to acknowledge J.R. de Jong for technical support and S.M.M. Boerdijk, Y.A.M. van der Knaap, J.G. Streurman-Werdekker and J. Wiegers for the MAC and CAC data reconstructions.

References

Andersson, J. L., Vagnhammar, B. E., Schneider, H. (1995). Accurate attenuation correction despite movement during PET imaging. *J. Nucl. Med.* 36, 670–678.

Bergström, M., Bohm, C., Ericson, K., Eriksson, L., Litton, J. (1980). Corrections for attenuation, scattered radiation and random coincidences in a ring detector positron emission transaxial tomograph. *IEEE Trans. Nucl. Sci.* 27, 549–554.

Bettinardi, V., Pagani, E., Gilardi, M. C., Landoni, C., Riddell, C., Rizzo, G., Castiglioni, I., Belluzzo, D., Lucignani, G., Schubert, S., Fazio, F. (1999). An automatic classification technique for attenuation correction in positron emission tomography. *Eur. J. Nucl. Med.* 26, 447–458.

Brett, M., Bloomfield, P., Brooks, D. J., Stein, J. F., M., G. P. (1999). Scan order effects in PET activation studies are caused by motion artefact. *NeuroImage* 9, S56.

Friston, K. J., Ashburner, J., Poline, J. B., Frith, C. D., Heather, J. D., Frackowiak, R. S. J. (1995a). Spatial registration and normalization of images. *Hum. Brain Mapp.* 2, 165–189.

Friston, K. J., Frith, C. D., Liddle, P. F., Frackowiak, R. S. (1991). Comparing functional (PET) images: the assessment of significant change. *J. Cereb. Blood Flow Metab.* 11, 690–699.

Friston, K. J., Holmes, A. P., Worsley, K. J., Poline, J. P., Frith, C. D., Frackowiak, R. S. J. (1995b). Statistical parametric maps in functional imaging: a general linear approach. *Hum. Brain Mapp.* 2, 189–210.

Hoffman, E. J., Huang, S. C., Phelps, M. E., Kuhl, D. E. (1981). Quantitation in positron emission computed tomography: 4. effect of accidental coincidences. *J. Comput. Assist. Tomogr.* 5, 391–400.

Huang, S. C., Hoffman, E. J., Phelps, M. E., E., K. D. (1979). Quantitation in positron emission computed tomography: 2. effects of inaccurate attenuation correction. *J. Comput. Assist. Tomogr.* 3, 804–814.

Meikle, S. R., Dahlbom, M., Cherry, S. R. (1993). Attenuation correction using count-limited transmission data in positron emission tomography. *J. Nucl. Med.* 34, 143–150.

Nuyts, J., Dupont, P., Stroobants, S., Benninck, R., Mortelmans, L., Suetens, P. (1999). Simultaneous maximum a posteriori reconstruction of attenuation and activity distributions from emission sinograms. *IEEE Trans. Med. Im.* 18, 393–403.

Ollinger, J. M. (1992). Reconstruction-reprojection processing of transmission scans and the variance of PET images. *IEEE Trans. Med. Im.* 39, 1122–1125.

Phelps, M. E., Hoffman, E. J., Mullani, N. A., Ter-Pogossian, M. M. (1975). Application of annihilation coincidence detection to transaxial reconstruction tomography. *J. Nucl. Med.* 16, 210–224.

Siegel, S., Dahlbom, M. (1992). Implementation and evaluation of a calculated attenuation correction for PET. *IEEE Trans. Nucl. Sci.* 39, 1117–1121.

Talairach, J., Tournoux, P. (1988). Co-Planar Stereotaxic Atlas of The Human Brain. Thieme Verlag, Stuttgart.

Watson, C. C., Newport, D., Casey, M. E., deKemp, R. A., Beanlands, R. S., Schmand, M. (1997). Evaluation of simulation-based scatter correction for 3-D PET cardiac imaging. *IEEE Trans. Nucl. Sci.* 44, 90–97.

Weinzapfel, B. T., Hutchins, G. D. (2001). Automated PET attenuation correction model for functional brain imaging. *J. Nucl. Med.* 42, 483–491.

Zaidi, H., Diaz-Gomez, M., Boudraa, A., Slosman, D. O. (2002). Fuzzy clustering-based segmented attenuation correction in whole-body PET imaging. *Phys. Med. Biol.* 47, 1143–1160.